Mediterranean Archaeology and Archaeometry, Vol. 17, No 4, (2017), pp. 89-102

DOI: 10.5281/zenodo.893194

NOVEL APPROACHES IN SURFACE LUMINESCENCE DATING OF ROCK ART: A BRIEF REVIEW

Liritzis Ioannis[1], Panou Evangelia[1], Exarhos Mihalis[2]

[1]University of the Aegean, Dept. of Mediterranean Studies, Lab of Archaeometry & Lab of Environmental Archaeology, 1 Demokratias Str, Rhodes, Greece
[2]National Technical University of Athens, School of Electrical and Computer Engineering, Iroon Polytechniou 9, 15773, Athens, Greece

Received: 31/05/2017
Accepted: 21/11/2017
Corresponding author: I. Liritzis (liritzis@rhodes.aegean.gr)

ABSTRACT

The direct dating investigation of rock art remains a deficit issue yet the surface luminescence dating of rock surfaces initiated in the 90's has made some considerable progress. The luminescence dating of lithic surfaces inheres a dual mechanism regarding bleaching / growth of luminescent signal by depth and exposure time. The present overview reconfirms the suggestion that rock surfaces contain a record of exposure and burial history and that these events can be quantified. The physical mechanisms in trapping / de-trapping of electron traps, under different conditions of sun exposure and burial, the mathematical modeling of experimental and simulated data (modified double exponential and cumulative log-norm) and some World examples are briefly reviewed.

KEYWORDS: bleaching, solar, irradiation, chronology, monument, lithics, fitting, modelling, mechanism, exponential, log-norm

1. INTRODUCTION

The investigation of Rock art is highly stimulating, the carved images are made for millennia, enrich our experience, and can embellish our own art, culture, and existence. This art can help us create more myths about the past and we can invent our own favored story of what happened in that past. However, this way interpretations of rock art images intrigue and may lead one to pareidolia, attached with ethnographic and neuroscientific issues. Provided we indulge in the interpretation without physical interference with the rock art it is a perfectly harmless avocation. If in the process one does not underestimate any other culture or impose any damage on the rock art, quests regarding motivation of their making are plausible – as long as, we make no attempt of presenting them as science (Bednarik, 2013). Science enters the scene in their material analysis and documentation.

Here we present the surface luminescence dating of surface rocks as an upcoming novel technique of absolute dating.

The resetting of the luminescence signal on surfaces is made by exposure to solar radiation. Suitable rocks include sandstones, granites, marbles, limestones, schists and others that include quartz and feldspar minerals. Here two mechanisms prevail:

First, the surfaces exposed to the sun define the zero time, zero being the moment from which the surfaces are no longer exposed to sunlight, and the luminescence clock counts the time. The dating concerned the time the huge blocks were carved by ancient masons, placed on appropriate position on the wall being covered by another block, thus inner surfaces are not sun exposed until today. The exposure to sun is interrupted by the overlay masonry block. Thereafter the luminescence of the emptied traps (in first mm or so surface layer) grows by the time due to the irradiation by ionizing radiation of the environment (the rock itself, the surrounding media and the cosmic rays). In 1994 the first development of dating monuments was testing the novel approach on well-known dated Greek monuments (Liritzis, 1994). Measuring the inner surface between two blocks one calculates the time the wall was build. A review on this has been written by Liritzis (2011).

Secondly, in continually exposed rock surfaces (i.e. not superimposed by another block) a different version is followed for age calculation, based on the solar radiation continually erasing the electron traps in the minerals of the rock (quartz, feldspar). These traps are refilled by environmental radiation derived from natural radioisotopes of immediate vicinity of the rock sample. The bleached luminescence is a function of depth below surface, as well as, the duration that the surface is exposed to sun. The remaining luminescence as a function of depth on a rock surface is a mathematical function that includes the age or the sun exposed time from the moment of carving until today. If the continuous illuminated carved or painted rock surface due to various reasons falls into the ground covered by sediment overtime, the luminescence grows in first surface layers from surrounded ionizing radiation and the signal increases by time.

Some publications have been produced on the 'surface luminescence dating' SLD method. Indeed, the attenuation of sunlight through different rock surfaces and the thermoluminescence (TL) or Optical stimulated luminescence (OSL) residuals clock resetting derived from sunlight induced eviction of electrons from electron traps, is a prerequisite criterion for potential dating (Liritzis, 2011; Laskaris & Liritzis, 2011; Chapot et al., 2012; Liritzis et al., 2013a, 2014, 2015; Sohbati, 2013, Sohbati et al., 2015; Freiesleben et al., 2015).

A brief overview of the surface luminescence dating method especially for rock art will be presented with case studies and the advantages and limitations shall be discussed.

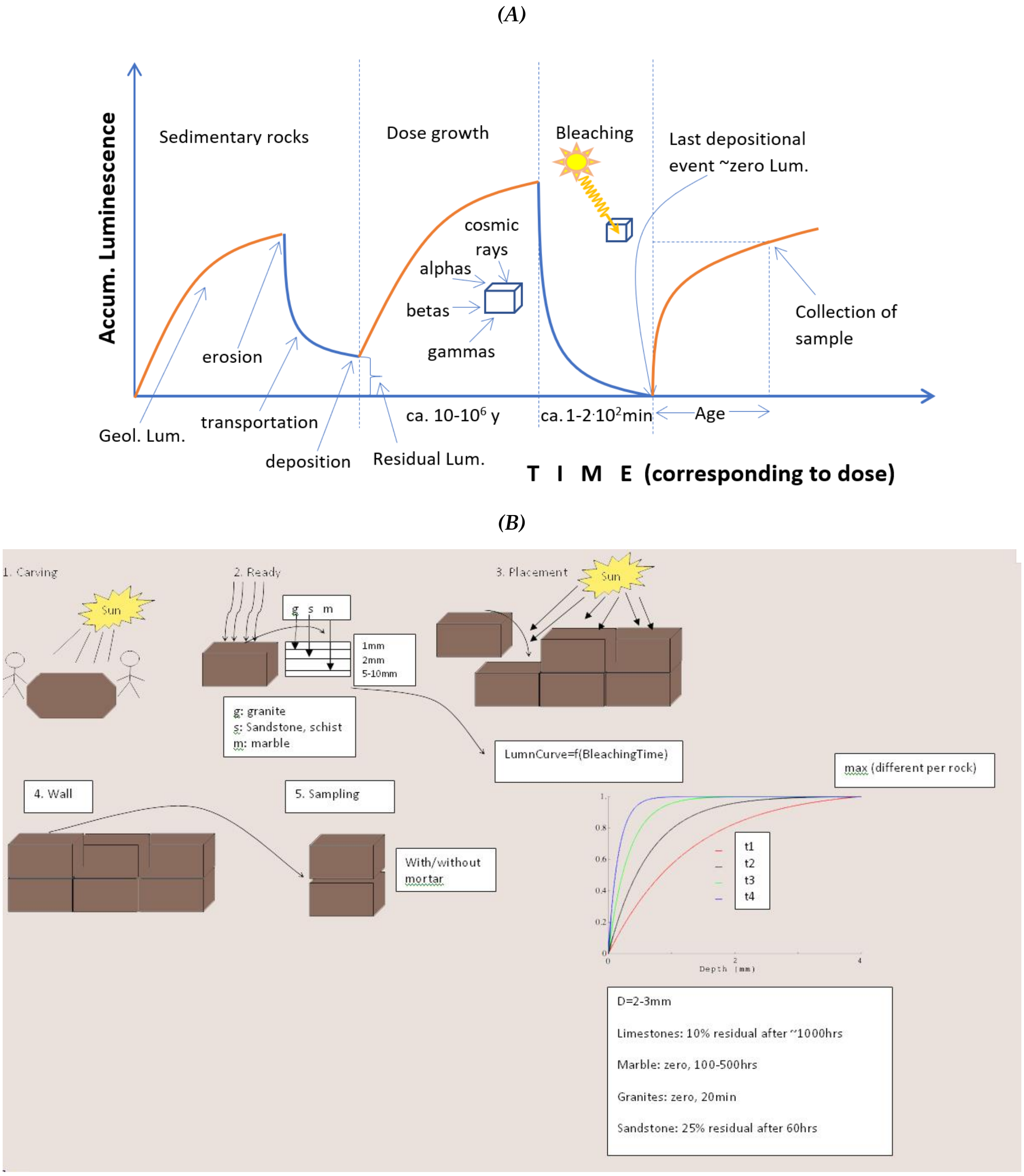

***Figure 1** Schematic diagram of luminescence dating of monuments, sediments or burnt structures (zero set by fire or sun exposure). Growth, resetting measurement. (A) Erosion, transport, deposition of sediments, then growth / build up of luminescence by environmental radiation (alphas, betas, gammas, cosmic rays), for 100 to millions of years, following possible exposure to sun (accidentally or intentionally) and reset (zero luminescence, empty traps) within minutes; and again growth of luminescence till today with sampling and measurement of the accumulated luminescence.*

(B) The five steps of surface luminescence dating in monuments 1. A stone block removed from a quarry carved and thus the surfaces exposed to sunlight, 2. that resets the clock to zero for the first mm or so upper layer of the block and depending from the rock type the complete bleaching takes a few minutes to some hours (marble, sandstone, granite). If the carving is made on a rock then the permanent sun exposure (if not fallen) will produce bleached curves versus depth as saturated exponential ones, the saturation level being the geological luminescence of rock at depth where sunlight can not reach or the exposure time is not enough to empty traps at that depth below surface. Bleached curves are a function of rock type, depth and exposure time (i.e. the age of rock carving) (Laskaris & Liritzis 2011; Liritzis et al., 2010; Vafiadou et al., 2007). 3. The carved block is placed in the appropriate place in the building, 4. The wall is made and block surfaces are no longer exposed to light and accumulate dose by time. 5. Today sampling of piece of rock that includes inner surface avoiding sun exposure and in the lab the total dose since building is measured. For rock art i.e. continually exposed rock surfaces to sunlight the D_e evaluation starts from step 2 straight to sampling step 5 and measurement (see below Figs. 3 & 4)

2. LUMINESCENCE. The Physics in Rock Art Archaeology

The luminescence physical phenomenon relates to the solid-state physics and nuclear physics (dosimetry) with ionizing radiation and absorbed doses, of valence/conductivity zones, the trapping sites which are imperfections of the lattice — impurities or defects of traps and holes or luminescent centers, and the energy level bands. The diagram illustrating the creation of luminescence centers in crystal lattices through exposure to ionizing radiation Irradiation-Storage-Eviction is shown in Fig.2.

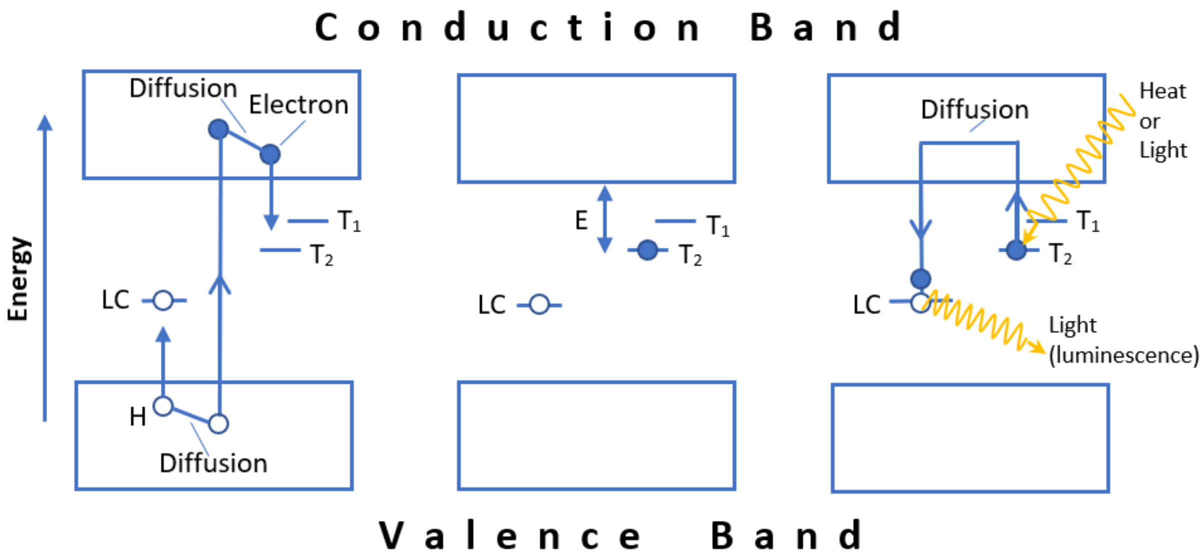

(a)
Irradiations by
Ionizing radiation

(b)
Storage of
electrons

(c)
Ejection of
electrons

Figure 2 Irradiation, storage and eviction of electrons. Energy levels in an insulator (mineral) with luminescent centers LC, electron traps T, holes (H)

Deep Electron Traps (high T) imply higher saturation levels, and shallow electron traps (low T) implies lower saturation level. The higher escape frequency results to de-trapping and recombination of electrons with holes or centers with evident emission of light (luminescence).

Trapped Electrons

During exposure to nuclear radiation, some bound electrons of the atoms making up a mineral's lattice are detached from their parent nuclei and become freely mobile and diffuse, trapped in holes or hole luminescent centers, and also enter the conduction band. Structural defects in the lattice (vacancies, interstitial atoms, and substitutional impurities, such as Frenkel and Schottky defects, Kittel 2005: *585–588*) create localized charge deficits, which act as traps T for the conduction electrons. Most electrons recombine or are briefly trapped in very shallow traps, but a few are trapped at deep traps and remain there over geological time-scales (1-1000 million years). The now charge-deficient ion hole, that contributed the trapped charge becomes a luminescence center LC (Fig. 2 A).

Recombination

Electrons trapped in deep traps T do not readily recombine unless induced to do so by complete natural bleaching i.e. "clock-resetting events", by heat or light or under strictly controlled laboratory conditions. Heat or light (e.g. LEDs) can eject charges from traps T back into the conduction band. When an electron recombines with a luminescence hole center LC, a photon is emitted. This phenomenon forms the basis of thermo-stimulated luminescence (TL) and optically-stimulated luminescence dating, OSL (Liritzis & Droseros, 2015).

The phenomenon underlying the thermo-stimulated luminescence (TSL) process is usually explained on the basis of band structure of electronic transition in an insulating material exhibiting TSL.

$$P = s \cdot e^{-E/KT} \tag{1}$$

P is the probability per second that the amount of energy is enough to release the trapped electron from its localized state (i.e. to overcome the trap energy barrier E and undergo a transition into the conduction band): 's' is frequency factor and is related to the local lattice vibration frequency and the entropy change associated with the charge release, 10^{12}-10^{14}/s, K Boltzmann's constant, T temperature.

The amount (and rate) of trapped electrons measure the accumulation, thus, time = age.

$$Age = \frac{\text{Total Accumulated Dose, } D_e}{\text{Annual Dose, } d_e} \tag{2}$$

Where D_e in Grays = 1000 mGys, and d_e the absorbed dose in one year from alpha particles, beta particles, gamma rays derived from natural environmental isotopes of U, Th, K, Rb, and cosmic rays dose rates (usually 1-5 mGy/year) (Liritzis et al., 2013b).

3. SOME CASE STUDIES

1) Marbles, marble schists and granites have been tested and dated by SLD, investigating the modeling of change of residual luminescence as a function of two variables, the solar radiation path length (or depth) and exposure time, which offer further insight into the dating concept (Liritzis et al., 2010). The double exponential function modeling based on the Lambert–Beer law, valid under certain assumptions, constructed by a quasi-manual equation fails to offer a general and statistically sound expression of the best fit for most rock types, and an improved double exponential model (Sohbati et al., 2015; Liritzis and Bakopoulos, 1997) was proposed applied to burial and (time) exposure events. A cumulative log-normal distribution fitting provides a satisfactory mathematical approximation for marbles, marble schists and granites, where absorption coefficient and residual luminescence parameters are defined per each type of rock or marble quarry (Laskaris & Liritzis, 2011). The new model is applied on available data and age determination tests.

The data regarding the shape of luminescence (either TL or OSL) drop due to sun bleaching or solar simulator for the marbles, schists and granites derived from the published sources have been examined for a best mathematical expression to describe their variation. In fact, searching for appropriate functions and based partially on the Lambert–Beer law but modeling variation of relevant luminescence phenomena too the error function (erf) was found, by trial and error, to offer the best simulation and fit. That is a double exponential based on Beer-Lambert law applied for the attenuation and rate of bleaching (evicting) electron traps by depth (see for example; Kreutzer and Dietze (2017). However, earlier investigation (Liritzis and Bakopoulos 1997) has shown that in the TL bleaching in calcites, the decay of residual TL after exposure to sunlight as a function of exposure time is described by an exponential de-excitation model. This may be a simple exponential or a double exponential (eq.3)

$$TL(t) = C_1 e^{-\lambda_1 t} + C_2 e^{-\lambda_2 t} + C_0 \tag{3}$$

Where C is a constant background.

Here the recombination (or de-excitation) rates for the photon emission (luminescence), λ_1 and λ_2, are related to the lattice defects in the crystal. For a discrete trap energy spectrum in the lattice, the luminescence L(t) curve is the sum of discrete exponential components. Moreover, the function occasionally behaves as a stretched exponential term: This means that electron de-excitation rate distribution value is proportional to the point defect distribution value on dV at a position (x, y, z). The above relationships indicate a fractal distribution of point defects in the crystal lattice (eq.4).

$$TL(t) = e^{-(\bar{\lambda} t)^{a}} \sim C_1 \int_0^\infty P(\lambda) e^{-\lambda t} \, d\lambda \tag{4}$$

where λ belongs to $[0, +\infty)$, and $\bar{\lambda}$ is the mean value of recombination (de-excitation) rates λ, which represent a continuous or fractal distribution of recombination centers in the crystal.

In fact based on the earlier rationale, the distribution of residual Tl or OSL luminescence signal, after bleaching, as a function of depth x, (for continuous exposure) follows the cumulative logarithmic normalized distribution, while attributing to coefficients a physical meaning (eq. 5):

$$TL(x; a, b, c, d) = a + \frac{b}{2} erfc\left(\frac{-\ln\left(\frac{x}{c}\right)}{d\sqrt{2}}\right) \tag{5}$$

where *a* is the residual luminescence, *b* is the geological minus residual, *c* is the transition depth of the residual TL curve and *d* is a non-dimensional factor, most probable a measure of the dispersion of the unbleached traps around the transition depth. From our research until now, this d factor seems to be uncorrelated with exposure time or transition depth. However, coefficient *c* (transition depth) exhibits a linear dependence on time when plotted against, the exposure time ln (days) denoted as t.

The generalized cumulative log-normal distribution equation (eq.6) finally becomes:

$$TL = 3.33 + 22.4 erfc\left(\frac{-\ln\left(\frac{x}{c}\right)}{0.3336}\right) \tag{6}$$

Eq. (6) represents the general equation for the Penteliko Marble (Attica, Greece), exploited quarry by ancient Athenians, and can be used in any future study of this material. The linear relationship between coefficient *c* and *time* – imply that residual TL depends on path length (depth below surface) and time exposure.

A demonstration of the experimental data for enteliko marble, Greece (circles) and the Cumulative Log-Norm curves of Eq. (5) with values of transition depth c as they were calculated from the Cumulative Log-Normal fitting is shown in Fig.3.

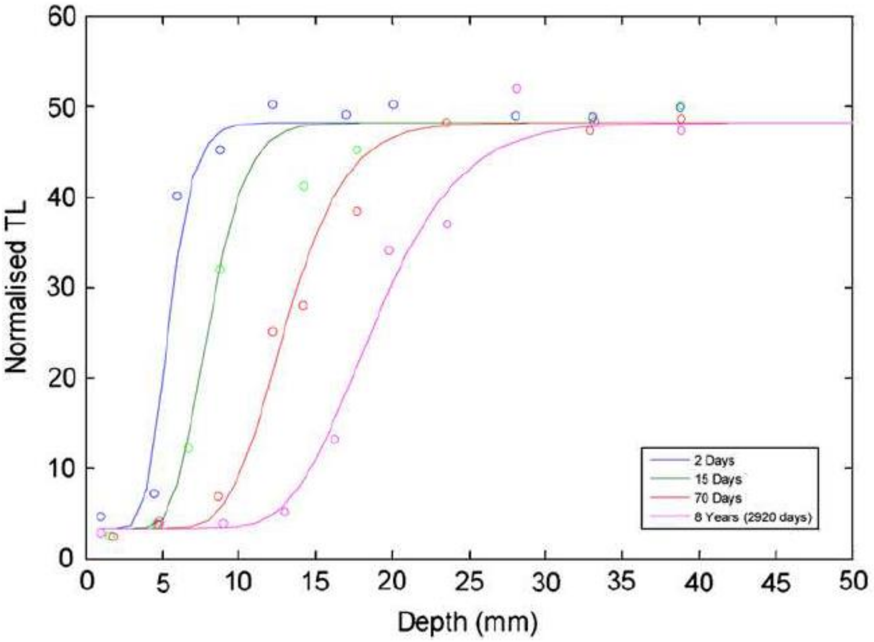

Figure 3 Bleached luminescence by depth in marble. Experimental data (dots) and fittings by Eq. (5) (solid curves) for exposure times from 2 days (far left) to 8 years (far right) (from Laskaris & Liritzis 2011, Fig.10).

Analysis of the outer 1 to 5 mm of a modern analogue sample may investigate if this surface had been sun exposed long enough for its residual luminescence signal to be reduced to negligible levels. Thus, for a rock art exposed to sun for some thousands of years, t_x, it has zero D_e, along a few mm from top surface, say d_x. Thereafter D_e increases exponentially towards saturation in deeper layers. After the long exposure period a fallen piece to the ground and covered by sediment, will exhibit a flat increase of D_e to the depth d_x and a non-linear increase beyond d_x to the saturation d_s depth (see Fig.4). In fact, the beta dose contribution in the about first mm will increase a bit the dose at the surface layer, thereafter the dose is constant to a depth x, the d_x. This flat D_e, beyond the first mm may determine the date the piece has fallen (Liritzis et al., 2017).

2) Optically stimulated luminescence (OSL) is used to determine the age of a rockfall event that removed part of the pictograph figures at the Great Gallery rock art panel in Canyonlands National Park, Utah, USA. It has been shown that OSL dating can determine the age of rockfall events by dating the concealed surface of either a fallen rock fragment or the underlying sediment

Analyses from the outer millimeter of the buried surface of a rockfall boulder and quartz grains from the underlying sediment both provide consistent ages that also agree with an AMS radiocarbon age of a cottonwood leaf found immediately between the clast and underlying sediment. Measurement of the OSL signals shows that there is no detectable increase in the OSL signal to a depth of at least 3 mm suggesting that the surface OSL signal was fully reset to this depth before burial, and burial time was not high. Consistent OSL and radiocarbon ages for this rockfall event provide a minimum age of ~900 years for the Great Gallery, which is the type locality of Barrier Canyon Style rock art with a controversial and unknown origin (Chapot et al., 2012).

3) From another attempt in Barrier Canyon Style (BCS) rock art in Canyonlands National Park, Utah, USA Sohbati et al. (2012) dated three rock samples. The shielded surface of the buried talus sample is decorated with rock art; this rock fell from the adjacent Great Gallery panel.

Two samples are from talus with unknown daylight exposure histories; one of these samples was exposed at the time of sampling and one was buried and no longer light exposed. A third sample is known to have been first exposed 80 years ago and was still exposed at the time of sampling. Cutting slices of 1mm thickness, First, the OSL-depth profile of the known-age sample is modeled to estimate material-dependent and environmental parameters. These parameters are then used to fit the model to the corresponding data for the samples of unknown exposure history. From these fittings it was calculated that the buried sample was light exposed for ca. 700 years before burial and that the unburied sample has been exposed for ca. 120 years. Related research using conventional OSL dating suggests that this rockfall event occurred ca. 900 years ago, and so they deduced that the rock art must have been created between ca. 1600 and 900 years ago (Sohbati et al., 2012).

4) The construction age of a pavement in a prehistoric cult site in Negev desert, Israel, is established by determining the burial age of: (a) a cobble used in the pavement, and, (b) the underlying sediment. In the OSL protocol the first IR stimulation at 50°C (IR50) was followed by a second IR stimulation at 225°C (pIRIR225). The quartz OSL age and the K-feldspar corrected IR50 age from the sediment and the corrected IR50 and pIRIR225 ages from the cobble surface are all consistent, and give an average age of 4.22 ± 0.06 kyr. Although the very similar ages indicate the reliability of the methods, these ages are ~3-4 kyrs younger than that expected for the sites of ca. 8th millennium BP. The IR50 and pIRIR225 luminescence-depth profiles from the cobble indicate multiple exposure and burial events in the depositional history These profiles were modelled with a multiple exponential function that encompasses bleaching and growth. The apparently young ages may represent a later intervention in the site during the late 3rd millennium B.C. (Sohbati et al., 2015).

In order to estimate the degree of bleaching of the cobble surface before the final emplacement in the pavement, one can use the fitted values of constructed equation to predict the shapes of the profiles resulting from the last exposure event immediately before burial. The predicted profiles show that the IR50 and pIRIR225 signals were almost certainly completely reset to depths of ~7 and ~2 mm, respectively, before the cobble was incorporated in the pavement. Thus, one can be confident that the D_e values measured from the surface slices do not include any poorly-bleached component (no significant residual doses) and, from that point of view at least, should be satisfactorily accepted.

5) In rock art dating research OSL is applied for D_e using IR or blue light emitting diodes (Liritzis & Droseros, 2015) for stimulation and different preheating protocols, as in conventional OSL of quartz and feldspars (Liritzis et al., 2013, p.10). On a simulating (hypothetical) case study the schematic diagram of Fig.4 shows the evolution of expected growth / bleached luminescence curves as a function of depth and time, say in a rock art, which follows the expected experimental luminescence bleaching by depth (Laskaris & Liritzis, 2013). For initial sun exposure period of a rock art image (e.g. cupules, grooves etc.) which lasts for a long-time period say t_1 the first exposure (1E) is produced; subsequent rock fall and the burial time from fallen piece the first burial (1B) curve is produced, and for a relatively short exposure to sun, curve 2E is obtained.

The 1E and 1B curves in Fig.4a are fitted by eq.5. The 1B plateau in fact defines the burial time and provides a *terminus post quem* for the age of rock art. In essence, the first millimeter or so surface layer will have an increased dose from betas in the attached sediment; the >1 mm layers experience on average a similar dose rate. The 2E curve more specifically, was accomplished using a double modified cumulative log-normal distribution equation (eq. 7) in order to take into account both the exposure and the burial event. That is, this was achieved by a recursive algorithm on all sets of data in order to achieve their best fit on the modified cumulative log-normal distribution. Figure 4(a) shows the resulting curves.

$$L(x; a, b_1, c_1, d_1, b_2, c_2, d_2) = a + \frac{b_1}{2} erfc\left(\frac{-\ln\left(\frac{x}{c_1}\right)}{d_1\sqrt{2}}\right) + \frac{b_2}{2} erfc\left(\frac{-\ln\left(\frac{x}{c_2}\right)}{d_2\sqrt{2}}\right) \qquad (7)$$

Table 1 contains the computed values of parameters a, b, c, d for each of these curves.

Thus, the fittings of these three curves are made by: a) a modified cumulative log-norm function, and, b) a double exponential concept using eq. 8 (for 1B and 1E) and eq.9 (for 2E, according to the similar modification of eq.5 to eq. 7), which lead to the cumulative log-normal for the three curves, such as, in Sohbati et al (2014, 2015); Laskaris and Liritzis (2011); Liritzis and Bakopoulos 1997) (Fig.4b).

$$L = R + Ce^{-\lambda_0 t e^{-kx}} \qquad (8)$$

$$L = R + C_1 e^{-\lambda_1 t_1 e^{-k_1 x}} + C_2 e^{-\lambda_2 t_2 e^{-k_2 x}} \qquad (9)$$

where R is the residual luminescence, C the bleached luminescence (geological minus residual), λ_0 is the time constant ($time^{-1}$) of the exponential decrease of luminescence as a function of time at surface, k_x is the rate of decrease of solar radiation in time at surface (x=0) or at depth x within the rock, with units (1/length), also called as attenuation coefficient of solar radiation (Beer–Lambert Law). These coefficients and constants refer to certain type of material and an electron trap i.e. TL peak or OSL component. Table 2 contains the computed values of the aforementioned coefficients for each of these curves.

Table 1: Coefficients of the modified Cumulative Log-normal equations 5, 7 (see, Fig.4a)

Set	a	b		C		d	
1B	0.2017	0.8071		6.966		0.2317	
1E	$3.802 \cdot 10^{-3}$	1.006		7.114		0.2239	
2E	$9.697 \cdot 10^{-3}$	1	2	1	2	1	2
		0.1926	0.8065	0.4625	6.9727	0.2552	0.2316

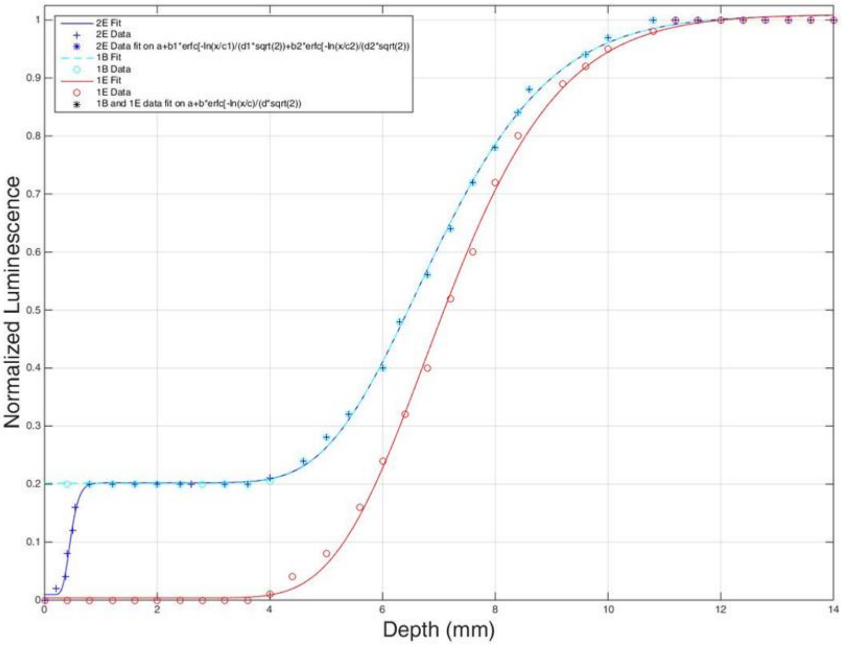

(a)

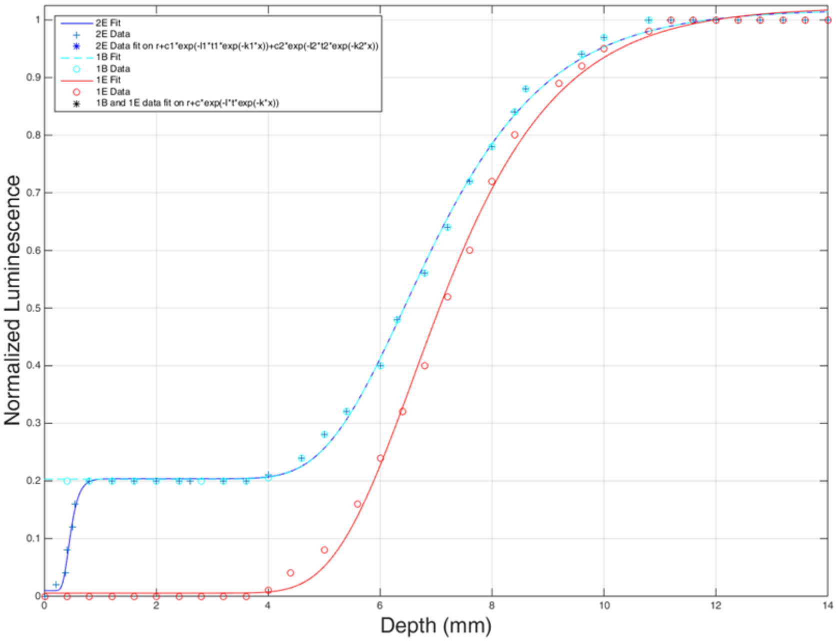

(b)

Figure 4: (a) Fitting of the simulated data using Log-normal cumulative distribution function reaching saturation at d_s, eq.5 and 7, (b) Fitting of the same data using double exponential function (eq. 8 and 9)

Table 2: Coefficients of the Double Exponential equation (eq. 8, 9)

<table>
<tr><th>Set</th><th colspan="2">C</th><th colspan="2">K</th><th colspan="2">$\lambda_i t_i$</th><th>R</th></tr>
<tr><td>1B</td><td colspan="2">0.8154</td><td colspan="2">0.6969</td><td colspan="2">88.82</td><td>0.2031</td></tr>
<tr><td>1E</td><td colspan="2">1.017</td><td colspan="2">0.7066</td><td colspan="2">105.7</td><td>$5.451 \cdot 10^{-3}$</td></tr>
<tr><td rowspan="2">2E</td><td>1</td><td>2</td><td>1</td><td>2</td><td>1</td><td>2</td><td rowspan="2">$9.697 \cdot 10^{-3}$</td></tr>
<tr><td>0.8146</td><td>0.1941</td><td>0.6976</td><td>9.626</td><td>89.35</td><td>59.15</td></tr>
</table>

Tables 3 and 4 contain the goodness of fit statistics for the cumulative log-normal distribution equation and the double exponential equation respectively. These tables indicate generally better matching of the cumulative log-normal distribution equation than the double exponential one.

Table 3: Error Values of fitness using Cumulative Log-normal model (eq. 5, 7)

Set	Sum of Squares	r^2	Adjusted r^2	Root mean squared
1B	$1.906 \cdot 10^{-3}$	0.9995	0.9995	$8.251 \cdot 10^{-3}$
1E	$3.541 \cdot 10^{-3}$	0.9994	0.9994	$1.105 \cdot 10^{-2}$
2E	$2.596 \cdot 10^{-3}$	0.9995	0.9994	$8.87 \cdot 10^{-3}$

Table 4: Error Values of Fitness using Double Exponential model (eq. 8, 9)

Set	Sum of Squares	r^2	Adjusted r^2	Root mean squared
1B	$3.901 \cdot 10^{-3}$	0.999	0.9988	$1.202 \cdot 10^{-2}$
1E	$7.134 \cdot 10^{-3}$	0.9989	0.9987	$1.596 \cdot 10^{-2}$
2E	$4.615 \cdot 10^{-3}$	0.9992	0.9989	$1.222 \cdot 10^{-2}$

At any rate the trap filling rate F(x) depends on the dose rate in the situation under consideration. The variation of dose rate with depth into the rock must also be taken into account because of the difference between radionuclide concentrations, and/or water contents at the rock/sediment or rock/air interface. For a rock art usually vertical in situ, water uptake at the surface is assumed negligible. But during burial the sediment contributes beta rays dose rate to the outer layers of 1 mm, thereafter the dose comprises from the rock internal radioactivity and the gamma ray dose rate of surrounding sediment. Thus, avoiding the outer about 1 mm with a usually patina coating there is no variation in beta radiation with depth into the rock sample for a rock sample buried in sediment. Note these are dose rates to the average matrix. Additional dose rate comes from cosmic radiation (not significantly dependent on depth into rock surface over the centimeter scales considered here) and internal depth-independent uranium, thorium and potassium inclusions are added and modifications for the effect of grain attenuation are taken into account. To calculate the dose rate in a given depth interval x_1 to x_2, the depth-independent dose rate is negligible except if inhomogeneity is noticed within the rock (see, Freiesleben et al., 2015). Briefly the trapping and de-trapping of electron traps in rock art minerals by ionizing radiation and light exposure respectively are different processes for a rock art exposed surface in situ and for a fallen piece into sediments. The instantaneous trapped charge concentration (electrons in trap lattice defect points) at depth x is n(x,t) and the available concentration sites are N(x) with a trap filling rate F(x), which is proportional to dose rate d(x) (which for homogeneous radiation field around a fallen rock is constant), and inversely proportional to a filling rate constant f_o, i.e. $F(x) = d(\chi) / f_o$.

In sun exposed rock surface the filling rate F(x) in traps at depth χ is due solely to the radioactivity of rock itself (+ cosmic rays). While E(x) the rate of emptying of traps at depth χ due to sunlight (exponentially decreased in an analogue manner of exponential fall of solar radiation attenuated by depth), is a product of solar flux photons φ(λ,x) and the photoionization cross section σ(λ, Z) for an average solar spectrum present at χ=0, i.e. rate of ionization is φ,σ and rate of emptying $E(\chi) = \varphi \cdot \sigma \cdot e^{-\mu x}$, where μ the attenuation coefficient (as in eq. 6 above).

The trapping and de-trapping of electrons during radiation and light exposure

The solar photon flux impinging into the rock art surface is defined by next equation (10) as number of photons per unit time and rock area:

$$\Phi = \frac{\#\,\text{of photons}}{\sec \text{m}^2} \qquad (10)$$

As the solar photon flux does not give information about the energy (or wavelength) of the photons, the energy or wavelength of the photons in the sun must also be specified on an average spectrum. At a given wavelength, the combination of the photon wavelength or energy and the photon flux at that wavelength can be used to calculate the *power density* for photons at the *particular wavelength*. The power density is calculated by multiplying the photon flux by the energy of a single photon. Since the photon flux gives the number of photons striking a surface in a given time, multiplying by the energy of the photons comprising the photon flux gives the energy striking a surface per unit time, which is equivalent to a power density. To determine the power density P in units of W/m^2, as proportional to flux, Planck constant, light speed and inversely proportional to wavelength, λ, the energy of the photons must be in Joules. The equation is:

$$\text{P}(\text{W/m}^2) = \varphi\frac{\text{hc}}{\lambda} \qquad (11)$$

Upon sunlight exposure not every photon which encounters an atom or ion will photoionize it. This is the phenomenon in which the absorption of electromagnetic radiation by an atom in a mineral induces the atom to emit a bound electron and thereby become ionized. The probability of photoionization is related to the *photoionization cross-section*, which depends on the energy of the photon and the target being considered, σ (E or λ, Z). For photon energies below the ionization threshold, the photoionization cross-section is near zero. As expected the photoionization cross-section decreases as the photon energy increases (or as λ decreases) (Chang & Fang, 1995). The Photoionization cross section is not an easy task and most ab initio theoretical models have successfully calculated outer p-subshell photoionization cross sections of the rare gases by treating in their alternative ways the key interactions described elsewhere, i.e. the particle – hole interactions (Starace, 1988).

Thus photoionization is the probability per unit area, per unit time that a photon of a given energy can be absorbed by an atom to excite the photoelectrons. The fictitious area representing the fraction of incoming photons that will be absorbed in the photoionization process is given below while the units are barns (10^{-24} cm^2), eq.12 below;

$$\text{cross section} \nearrow \sigma(h\nu) = \frac{P(h\nu) \longleftarrow \text{no of photons absorbed per unit time}}{I(h\nu) \longleftarrow \text{Incident photon flux}} \qquad (12)$$

That is eq. 8 and 9 are deduced from the combination of exponential Lambert-Beer law and the resulted exponential decrease of emptying traps by depth E(x) where each parameter has a physical significance. Note that the trap filling during daylight exposure is ignored near to the carved rock surface exposed to light but this does not apply at deeper layers within the rock where the E(x) tends to zero. This gradual bleaching of luminescence quantified as a function of depth produces family sigmoid-like saturating exponential curves shifted with depth corresponding to certain sun exposure times. That is the obtained curve represents the time elapsed since carving of the rock surface to make the rock art.

The deduced multiple double exponential and respective parametrization by Freiesleben et al. (2015) and Sohbati et al. (2015, eq.3) are similar to figures above. In fact, their experimental data are fitted equally well by our eq. (7) above (Fig.5).

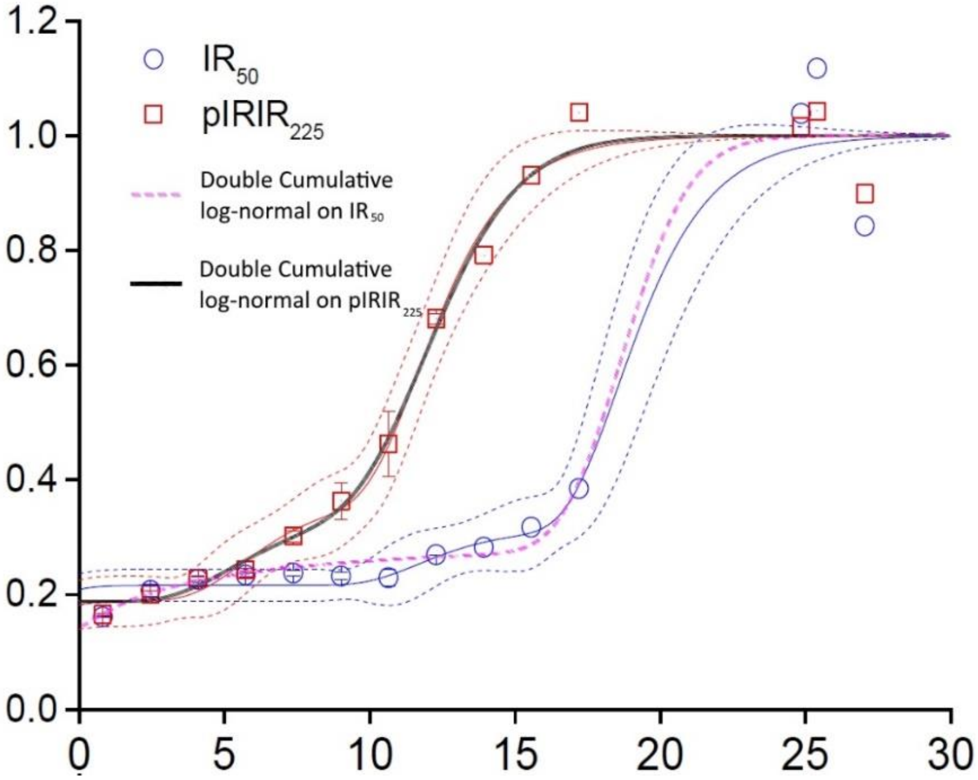

Figure 5 Fitting of experimental data (Sohbati et al., 2015), by their proposed multiple exposure and burial events model of luminescence versus depth, as squares and circles applying two protocols for D_e, the solid red line with associated red dashed 95% confidence lines, and blue solid line with red dashed 95% confidence lines, compared with the cumulative double log-normal, black solid and dashed pink lines, respectively.

1) Surface luminescence dating of ancient buildings, walls, threshing flat stones, and other stone blocks with or without association to sediment cover and other datable material, have been dated with success (Liritzis et al., 2013b).

A typical case study of Surface luminescence by OSL dating is a fortified wall at prehistoric settlement of Strofilas, Andros Island in the Aegean Sea. A Final Neolithic to Early Cycladic period has been assigned regarding masonry, fortification, and richly engraved rock art, dated by OSL of walls and SIMS-SS of obsidian hydration dating. However, the inscribed ships (Fig. 6) rather belong to the same cultural phase of end of 4th millennium BC. In fact, luminescence yields an average date of 3520 (±540) BC and the Obsidian an average date of 3400 (±200) years BC, both of which, within overlapping errors, suggest the main settlement occurred during the Final Neolithic (Liritzis, 2010).

However, the engraved vessels on some façade of flat rocks in the masonry could well be dated by the abovementioned techniques, but the coverage by sediment could present some problem, which theoretically could be tackled by example 5 above (Fig.4, curve 2E), but sampling is not allowed.

It suffices to say that some carving forms (e.g. boats) boats were remade to update the boat style so that it corresponded with what was current in a period that was later than when it was first cut. Thus, it is vital the need for more in-depth studies to understand the creation and use of rock art over an extended period. It is argued that rock art sites are connected to social traditions that made people return to the same place and make changes to already existing images (Milstreu, 2017).

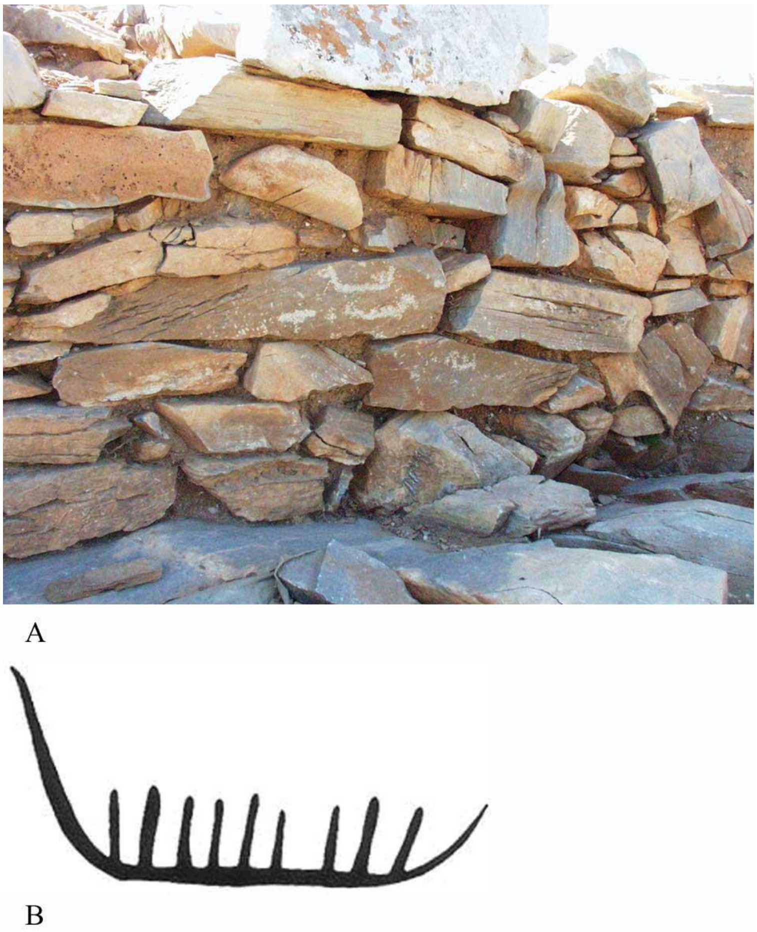

Figure 6. Part of the fortified wall of Strofilas settlement showing carved vessels (A), and a reproduced image of ship (B) (from Liritzis 2010).

4. DISCUSSION - CONCLUSION

The dating of rock art is upcoming. Certainly, more applications are needed, but the rationale for the luminescence history profiles in rock surfaces have been quite well established. The errors involved as in OSL dating refer to the dose rates and especially here the equivalent dose De. Cutting slices or removing powder is a delicate matter and requires further attention. The surface of the rock fragment is first cleaned with diluted HCl. This surface is then lightly abraded in 1 mm increments up to a depth of 12 mm (12 subsamples) using a medium coarse rasp (#100). The abraded grains of gentle plating of all subsamples are treated with acetone. No acid treatment was made thus alphas are included in the dose rate. Care should be exerted in the removed powder to avoid intermixed grains from adjacent layers and blackening of rasp. Using new files powder can be removed per 100 scratch passes in a depth of 12 mm that corresponds to ~4 layers per mm or 0.25 mm /layer.

The fitted experimental data of luminescence versus depth from a rock surface follow a double exponential and/or a Log-Norm (erf) function, but this requires a further insight for future cases, and that both become easily accessible by other workers. The upcoming dating method is promising and the future development is anticipated to thrust forward the method and the rock art research.

ACKNOWLEDGEMENTS

IL thanks Dr R Bednarik with insightful discussions, Dr Kaltham Ali Al-Ghanim the Director of the Center for Humanities and Social Sciences, Qatar University and the Qatar University for inviting me to the Rock Art conference and we thank 2 anonymous referees for useful comments.

REFERENCES

Bednarik, R.G. (2013) On the neuroscience of rock art interpretation. *Time and Mind.* 6(1), 37-40.

Chapot, M.S, Sohbati, R., Murray, A.S, Pederson, J.L., Rittenour, T.M. (2012) Constraining the age of rock art by dating a rockfall event using sediment and rock-surface luminescence dating techniques. *Quaternary Geochronology.* 13, 18-25.

Freiesleben, T., Sohbati, R., Murray, A., Jain, M., al Khasawneh, S., Hvidt, S., Jakobsen, B. (2015) Mathematical model quantifies multiple daylight exposure and burial events for rock surfaces using luminescence dating. *Radiat. Meas.* 81, 16-22, http://dx.doi.org/10.1016/j.radmeas.2015.02.004

Kreutzer, S., Dietze, M. (2017) plot_GrowthCurve: Fit and plot a growth curve for luminescence data (Lx/Tx against dose). Function version 1.9.5. In: Kreutzer, S., Dietze, M., Burow, C., Fuchs, M.C., Schmidt, C., Fischer, M., Friedrich, J. (2017). Luminescence: Comprehensive Luminescence Dating Data Analysis. R package version 0.7.5. (https://CRAN.R-project.org/package=Luminescence)

Kittel, Ch. (2005) *Introduction to Solid State Physics* (8th ed.). Wiley.

Laskaris, N. & Liritzis, I. (2011) A new mathematical approximation of sunlight attenuation in rocks for surface luminescence dating. *J. of Luminescence.* 131, 1874- 1884.

Liritzis I., Bakopoulos Y. (1997) Functional behaviour of solar bleached thermoluminescence in calcites. *Nuclear Instruments and Methods B*, 132, 87-92

Liritzis (1994) A new dating method by thermoluminescence of carved megalithic stone building. *Comptes Rendus (Academie des Sciences*), Paris, 319 (serie II), 603-610.

Liritzis., I. (2010) Strofilas (Andros Island, Greece): New evidence of Cycladic Final Neolithic dated by novel luminescence and Obsidian Hydration methods. *Journal of Archaeological Science.* 37, 1367- 1377.

Liritzis, I., Polymeris, G. and Zacharias, N. (2010) Surface luminescence dating of 'Dragon Houses' and Armena Gate at Styra (Euboea, Greece). *Mediterranean Archaeology & Archaeometry, Special Issue* (D.Keller, guest editor) 10(3), 65-81.

Liritzis, I. (2011) Surface dating by luminescence: An Overview. *Geochronometria.* 38(3), 292-302.

Liritzis, I., Vafiadou, A., Zacharias, N., Polymeris, G.S. and Bednarik, R.G. (2013a) Advances in surface luminescence dating: some new data from three selected Mediterranean sites. *Mediterranean Archaeology & Archaeometry.* 13(3), 105-115.

Liritzis, I., Singhvi, A.K., Feathers, J.K., Wagner, G.A., Kadereit, A., Zacharias, N. and Li, S.-H. (2013b) *Luminescence Dating in Archaeology, Anthropology and Geoarchaeology: An Overview*. Springer Briefs in Earth System Sciences (http://link.springer.com/content/pdf/10.1007/978-3-319-00170-8.pdf)

Liritzis, I. & Vafiadou, A. (2014) Surface luminescence dating of some Egyptian monuments. *Journal of Cultural Heritage.* 16, 134-150.

Liritzis, I., Aravantinos. V., Polymeris, G.S., Zacharias, N., Fappas, I., Agiamarniotis, G., Sfampa, I.K., Vafiadou, A. and Kitis, G. (2015) Witnessing prehistoric Delphi by Luminescence dating. *Comptes Rendus PALEVOL.*14, 219-232.

Liritzis, I. & Droseros, N. (2015) Light emitting diodes and Optically Stimulated Luminescence dating in Archaeology: An overview. *Mediterranean Archaeology & Archaeometry*. 15(2), 277-291.

Liritzis, I., Bednarik, R., Polymeris, G., Iliopoulos, I., Zacharias, N., Kumar G., Vafiadou, A. and Bratitsi, M. (2017) *Daraki-Chattan rock art constrained OSL chronology: A first approach* (in preparation).

Milstreu, G. (2017) *Re-cut rock art images* (with a special emphasis on ship carvings). In Bergerbrant, S and Anna Wessman, A (editors) "New Perspectives on the Bronze Age Proceedings of the 13th Nordic Bronze Age Symposium held in Gothenburg 9th to 13th, 2015", Archaeopress Publishing Ltd, Oxford.

Chang, T.N. and Fang, T.K. (1995) Wavelength dependence of the nonresonant photoionization cross section of a two-electron atom near the ionization threshold. *Physical Review A*. 52 (3), 2052-2076.

Sohbati, R. (2013) *Luminescence, Rock Surfaces*. Encyclopedia of Scientific Dating Methods, Springer Science+Business Media Dordrecht, 10.1007/978-94-007-6326-5_83-4, 1-7.

Sohbati, R., Murray, A.S., M. S. Chapot, Jain, M. and Pederson, J. (2012), Optically stimulated luminescence (OSL) as a chronometer for surface exposure dating, *J. Geophys. Res.,* 117, B09202, doi:10.1029/2012JB009383.

Sohbati, R., Murray, A.S., Porat, N., Jain, M. and Avner, U. (2015) Age of a prehistoric "Rodedian" cult site constrained by sediment and rock surface luminescence dating techniques. *Quaternary Geochronology*. 30, 90-99.

Starace, A. (1988) *The Calculation of Photoionization Cross Sections*, Anthony F. Starace Publications 129, University of Nebraska – Lincoln Digital Commons@University of Nebraska, Research Papers in Physics and Astronomy, 1-12.

Vafiadou, A, Murray, A.S. and Liritzis, I. (2007) Optically Stimulated Luminescence (OSL) dating investigations of rock and underlying soil from three case studies. *Journal of Archaeological. Science.* 34, 1659-1669.